Continuous 2D trajectory decoding from attempted movement: across-session performance in able-bodied and feasibility in a spinal cord injured participant

Pulferer, Hannah S; Ásgeirsdóttir, Brynja; Mondini, Valeria; Sburlea, Andreea I; Müller-Putz, Gernot R

Published in:
Journal of Neural Engineering

DOI:
10.1088/1741-2552/ac689f

Continuous 2D trajectory decoding from attempted movement: across-session performance in able-bodied and feasibility in a spinal cord injured participant

Journal of Neural Engineering

PAPER

Continuous 2D trajectory decoding from attempted movement: across-session performance in able-bodied and feasibility in a spinal cord injured participant

Hannah S Pulferer[1], **Brynja Ásgeirsdóttir**[1], **Valeria Mondini**[1], **Andreea I Sburlea**[1,3] and **Gernot R Müller-Putz**[1,2,*]

[1] Institute of Neural Engineering, Graz University of Technology, Stremayrgasse 16/IV, 8010 Graz, Austria
[2] BioTechMed Graz, Graz, Austria
[3] Bernoulli Institute of Mathematics, Computer Science and Artificial Intelligence, Faculty of Science and Engineering, University of Groningen, Groningen, The Netherlands
* Author to whom any correspondence should be addressed.

E-mail: gernot.mueller@tugraz.at

Keywords: electroencephalography, trajectory decoding, learning effects, source localization, motor control, neuroplasticity, brain-computer interface

Supplementary material for this article is available online

OPEN ACCESS

RECEIVED
22 December 2021

REVISED
31 March 2022

ACCEPTED FOR PUBLICATION
19 April 2022

PUBLISHED
9 May 2022

Abstract

Objective. In people with a cervical spinal cord injury (SCI) or degenerative diseases leading to limited motor function, restoration of upper limb movement has been a goal of the brain-computer interface field for decades. Recently, research from our group investigated non-invasive and real-time decoding of continuous movement in able-bodied participants from low-frequency brain signals during a target-tracking task. To advance our setup towards motor-impaired end users, we consequently chose a new paradigm based on attempted movement. *Approach*. Here, we present the results of two studies. During the first study, data of ten able-bodied participants completing a target-tracking/shape-tracing task on-screen were investigated in terms of improvements in decoding performance due to user training. In a second study, a spinal cord injured participant underwent the same tasks. To investigate the merit of employing attempted movement in end users with SCI, data of the spinal cord injured participant were recorded twice; once within an observation-only condition, and once while simultaneously attempting movement. *Main results*. We observed mean correlations well above chance level for continuous motor decoding based on attempted movement in able-bodied participants. Additionally, no global improvement over three sessions within five days, both in sensor and in source space, could be observed across all participants and movement parameters. In the participant with SCI, decoding performance well above chance was found. *Significance*. No presence of a learning effect in continuous attempted movement decoding in able-bodied participants could be observed. In contrast, non-significantly varying decoding patterns may promote the use of source space decoding in terms of generalized decoders utilizing transfer learning. Furthermore, above-chance correlations for attempted movement decoding ranging between those of observation only and executed movement were seen in one spinal cord injured participant, suggesting attempted movement decoding as a possible link between feasibility studies in able-bodied and actual applications in motor impaired end users.

1. Introduction

High spinal cord lesions due to accidents or neurological disorders leading to a deterioration of the motoric abilities severely limit the motor function, and thus, overall quality of life, of the person affected (Charlifue *et al* 2012, Tulsky *et al* 2015). Ranging from restricted hand or arm movement to actual tetraplegia, completing everyday tasks may pose an insurmountable obstacle, and offering these people possibilities to regain motor control has been a focus of brain-computer interface (BCI) research for years

(Pfurtscheller *et al* 2000, 2003, Müller-Putz *et al* 2005, Rupp *et al* 2005, Rohm *et al* 2013).

Per definition, BCIs exclusively rely on invasively or non-invasively acquired brain signals and offer a range of possible outputs that enable the users to interact with their environment without any prior neuromuscular activity. Accordingly, BCIs intrinsically offer motor-impaired people the possibility of operating an end-effector (e.g., robotic limb, neuroprosthesis, etc) solely based on their brain activity, and thus provide an opportunity to regain independence (Rohm *et al* 2013).

Over the last decades, a broad range of tasks has been devised to investigate the neural correlates of specific movements non-invasively, ranging from basic right-vs-left-hand or foot classification tasks to increasingly complex paradigms in both able-bodied and spinal cord injured participants (Pfurtscheller *et al* 2000, 2009, Wolpaw and McFarland 2004, Shan *et al* 2015, Meng *et al* 2016, Müller-Putz *et al* 2016). However, the disparity between a mental task devised for control and the intended task at hand often makes the operation of BCIs unintuitive, apart from introducing a mental workload that is disproportionate to the intended action. As a result, recent research in the field has turned to BCI solutions offering more natural control to the user; in particular, solutions which allow unrestricted eye movements as can be expected also from everyday situations, as well as intuitive paradigms that connect the task in a straight-forward way with the intended goal (Ofner and Müller-Putz 2012, Müller-Putz *et al* 2016, 2018, 2022, Edelman *et al* 2019, Mondini *et al* 2020).

As has been demonstrated, decoding coordinates corresponding to intended movement via neural correlates intracortically or epidurally is feasible (Black *et al* 2003, Mulliken *et al* 2008, Hochberg *et al* 2012, Hammer *et al* 2013); however, over the last decade, research from various groups confirmed that kinematic information may also be inferred non-invasively. Within center-out tasks, the feasibility of decoding movement kinematics was shown both in offline (Bradberry *et al* 2010, Antelis *et al* 2013, Úbeda *et al* 2017) and online settings (Bradberry *et al* 2011, Korik *et al* 2019). Recently, the feasibility of decoding continuous movement within pursuit-tracking tasks in an online setting has been shown in a number of studies (Edelman *et al* 2019, Martínez-Cagigal *et al* 2020, Mondini *et al* 2020, Kobler *et al* 2020c). Devising specific 2D target-tracking tasks that ensured decorrelation between the two coordinates, our group recently reported correlations well above chance level during continuous trajectory decoding from low-frequency electroencephalographic (EEG) signals for executed movement in able-bodied participants (for a review see (Müller-Putz *et al* 2022)). Using partial least squares (PLS) regression followed by smoothing via unscented Kalman filter (UKF), correlations between depicted and decoded trajectories of on average 0.42 could be observed (Martínez-Cagigal *et al* 2020). In a similar task, the participants were instructed to observe the target only, leading to reduced, though still better than random, correlations of on average 0.31 (Kobler *et al* 2020c).

The previously mentioned studies were tailored to executed movement performed by able-bodied participants. However, actual end users experiencing severely limited motor output would have been unable to train the decoder by performing actual upper limb movement. Consequently, the objective of the current study was twofold. First, to cater the setup to motor-impaired end users to render non-invasive continuous movement decoding possible for persons with severe limitations in motor output as well. In this regard, we investigated a paradigm based on attempted movement instead of executed movement, similarly to (López-Larraz *et al* 2012, Ofner *et al* 2019). As there has been evidence that motor attempt (MA) tasks are perceived as more intuitive compared to motor imagery (MI) tasks by the participants (Müller-Putz *et al* 2019), in addition to leading to significantly higher BCI accuracies when classified against a rest condition (Chen *et al* 2021), we specifically chose attempted movement over MI e.g. employed in (Bradberry *et al* 2011, Korik *et al* 2018). A pilot study (Müller-Putz *et al* 2021) showed that continuous decoding from attempted movement is possible with above-chance correlations ranging between observed and executed movement. Additionally, the perceived level of control over the BCI at the beginning and at the end of the measurement suggested a possible positive impact of user training on the decoding performance of the interface. Thus, the second and final objective was to investigate improvements of the overall decoding performance over sessions.

As a result, in the current paper, we chose to investigate attempted movement performed within two different studies. First, the decoding performance during attempted movement in 2D trajectory decoding in ten able-bodied participants over three sessions within five days was analyzed. Preliminary results, limited to single-participant results exclusively evaluated in sensor space, have been published in (Pulferer *et al* 2021). The time frame of five days was chosen to offer the participants the possibility of recuperating from the mental workload imposed by the paradigm from one session to the next, while keeping the experience fresh in the participants' minds. During each session, two different paradigms were presented, which we evaluated in terms of changing decoding performance over time both in sensor space and in source space. And second, the feasibility and decoding performance in an spinal cord injury (SCI) participant within two different sessions, comprising an observation and an attempted movement task, respectively, were examined.

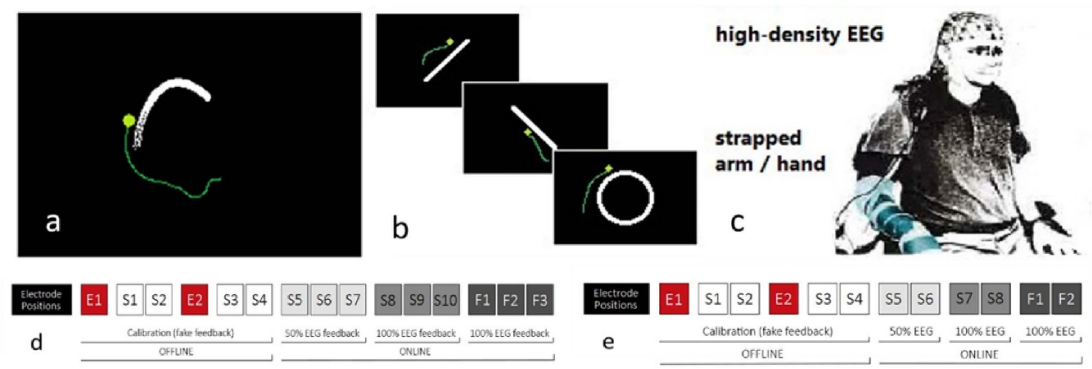

Figure 1. Paradigms and experimental setup. (a) Snakeruns (tracking task): black screen with moving white target (*snake*). (b) Freeruns (tracing task): static white shape (diagonal 1, diagonal 2 or circle) shown on screen to be traced at the participants' own pace. In both paradigms, online feedback in the form of the partially (50% EEG feedback condition) or fully (100% EEG feedback condition) EEG-decoded trajectory was delivered (green dot). (c) Experimental setup with the participant's dominant arm strapped to the arm rest during recording. Below, the measurement pipelines for able-bodied (d) and spinal cord injured (e) participants are shown (E: eyerun, S: snakerun, F: freerun).

2. Methods

2.1. Participants

EEG signals of each ten able-bodied participants (24 (mean) ± 5 (SD) years, five male) were recorded within three sessions over five days. The participants underwent a handedness test according to the Edinburgh Handedness Inventory (Oldfield 1971) prior to the first measurement, confirming right-handedness in each participant. Among the participants, four had previous experience regarding EEG measurements, though all of them were naive BCI users in terms of motor decoding. Additionally, each participant had normal or corrected-to-normal vision. Data of an eleventh participant (female) were excluded from further analysis due to erroneous marker-labeling during session 1. Each of the participants gave their written informed consent and received compensatory payment for participating in this study. The measurements were conducted as a part of the 'Feel Your Reach' project and as such were approved by the ethics committee of the Medical University of Graz (votum number 32–583 ex 19/20).

2.2. Data acquisition

During each measurement session, data were recorded on 64 channels (actiCAP, Brain Products GmbH, Gilching, Germany) consisting of a 60 channel EEG located according to the international 10–10 system and four electrooculographic (EOG) electrodes placed on the outer canthi of both eyes as well as above and below the left eye (see figure S1, supplementary material available online at stacks.iop.org/JNE/19/036005/mmedia). To allocate electrodes to the EOG, EEG channels at positions Fp1, Fp2, FT9, FT10 were removed. Additionally, the electrodes at TP9 and TP10 were relocated to positions PPO1h and PPO2h according to the 10–5 system for increased signal density in the parieto-occipital area, which has since been established to be of paramount importance for motor decoding (Wenderoth *et al* 2005, Mulliken *et al* 2008). Ground and reference electrodes were placed at Fpz and on the right mastoid for all participants. All data were recorded and synchronized using lab streaming layer (https://github.com/sccn/labstreaminglayer). The paradigms, as devised in (Mondini *et al* 2020, Müller-Putz *et al* 2021), were presented using a combination of MATLAB scripts (MATLAB 2015b, MathWorks Inc. USA) and Psychtoolbox (Brainard 1997, Pelli 1997, Kleiner *et al* 2007).

2.3. Paradigms

For each session, the participants were seated comfortably in front of a TV screen. To minimize the participants' range of motion and mimic attempted movement as demonstrated in primate studies (Velliste *et al* 2008), the dominant arm was strapped to the arm rest as shown in figure 1(c), largely restricting the possible motor output (Ofner *et al* 2019). The participants were instructed to attempt to move their lower arm as if wielding a computer mouse. As such, forward and backward movement of the arm was projected to upward and downward movement on screen. However, any actual motor output in the form of overt movement was prevented by the contraption encasing the limb. This approach was chosen because it was perceived as more intuitive than e.g., MI tasks by participants (Chen *et al* 2021). Additionally, it closely mimics the limitations in motor function which people with SCI experience: even though actual movement is desired, the motor output is eventually blocked.

Each session (see measurement pipeline in figures 1(d) and (e)) consisted of an offline calibration part, covering data acquisition for fitting the artifact removal (Kobler *et al* 2019, Kobler *et al* 2020b) and decoder (Martínez-Cagigal *et al* 2020) algorithms, and an online part, during which

feedback was provided in real time in two different feedback conditions (cf section 2.4).

2.3.1. Snakeruns

During the snakeruns, presented in both the offline (cf section 2.3.3) and the online part of the measurement, a white target (the snake) was shown on the black screen for a duration of 23 s per trial (figure 1(a)). As in (Mondini *et al* 2020), the snake trajectories were designed specifically to ensure decorrelation between x and y coordinates in order to allow a clear directional distinction between the decoded movement parameters. In addition to the snake, a green dot corresponding to feedback was depicted to provide the participants with immediate information on their performance. The participants were asked to track the snake with their gaze and simultaneously attempt movement of their strapped lower arm and hand as if wielding a computer mouse. As both target and feedback were shown at the same time, the participants had the opportunity to adjust their focus to try and increase the decoding performance, allowing them to learn to interact with the BCI in a constructive way.

2.3.2. Freeruns

In the freeruns, presented only in the online part of the measurement, the participants were confronted with one of three different white shapes on the TV screen (diagonals, circle) for 23 s per trial (figure 1(b)). The participants were instructed to trace the appearing shape with their gaze, as well as to attempt movement with their strapped limb like during the snakeruns. Again, they were asked to mainly focus on the target (in the case of the freeruns, the static shapes), though to keep the once again displayed green feedback dot in mind to adjust their approach with the goal of increasing their performance. To keep the task as intuitive and natural as possible, no additional instruction on how to proceed was given, apart from the premise not to pause at any point during the trial. Generally, the freeruns were designed as a self-paced paradigm, allowing the BCI users to freely operate the interface however they saw fit.

2.3.3. Calibration

During the offline calibration part, two eyeruns (38 trials, 8 s each) and four snakeruns (48 trials, 23 s each) were recorded (figures 1(d) and (e)). Data of the two eyeruns, corresponding to EEG and EOG signals recorded during resting gaze (12 trials), blinks (10 trials), horizontal and vertical eye movement (8 trials each), were subsequently used to fit models for attenuating eye artifacts as well as pops and drifts in the EEG channels during the following online part of the session (cf section 2.5). Finally, EEG data of the four snakeruns were used to fit the decoder model (cf section 2.6).

2.4. Feedback conditions

As data were still being acquired during the calibration phase, fake feedback (delayed snake) in the form of the green feedback dot was provided in the beginning. This followed the purpose of getting the participants acquainted with the additional visual information on screen from the start. After fitting the decoder model with the calibration run data, two different conditions of online feedback were introduced. First, the 50% EEG feedback condition was presented within three snakeruns (36 trials, 23 s each). Here, the green dot was depicted as the arithmetic mean of the target (snake) trajectory and the EEG-decoded positions. As the real feedback could vary noticeably from the depicted snake trajectory depending on the decoder performance, the EEG information was only weighted with 50% for the feedback at first to get the participants acquainted to the deviation and to avoid eliciting frustration. Afterwards, the 100% EEG feedback condition was introduced, during which the feedback dot position corresponded entirely to the EEG-decoded positions. For the first participant (P1), the 100% EEG feedback was exclusively delivered in the form of three freeruns, which afterwards (P2-P10) was expanded to three additional 100% EEG feedback snakeruns between the 50% EEG feedback snake runs and the 100% EEG feedback freeruns for additional quantitative analysis (see figure 1(d)). In contrast to the snakeruns that were completed prior, the freeruns were only presented in the 100% EEG feedback condition (figures 1(d) and (e)).

2.5. Data processing

After digitalization at an initial sampling frequency of 200 Hz, an anti-aliasing filter (25 Hz) was applied, and powerline noise was removed using a notch filter at 50 Hz. Subsequently, the signals were downsampled to 100 Hz and bad channels, identified by visual inspection, were interpolated from the signals of the four nearest channels, weighted with their inverse distance to the bad channel. With the acquired eyerun data, an eye artifact subtraction model was fitted for each participant using the SGEYESUB algorithm (Kobler *et al* 2020b) based on subspace subtraction to identify and attenuate the influence of saccades and blinks on the EEG. To additionally obviate an impact of potential residual eye-related activity on the EEG data, all channels within the most frontal (AF) row were excluded from further processing. Subsequently, the data were high-pass filtered at 0.18 Hz, re-referenced to the common average reference, and pops and drifts in the signals were attenuated using the HEAR algorithm (Kobler *et al* 2019, Kobler *et al* 2020b). After low pass filtering at 3 Hz and further downsampling to 20 Hz, the signals were fed to the decoder (Martínez-Cagigal *et al* 2020, Müller-Putz *et al* 2021), yielding the feedback output shown as a green dot on screen during the online runs.

2.6. Decoder

As in our previous studies (Martínez-Cagigal *et al* 2020, Mondini *et al* 2020, Kobler *et al* 2020c), the movement parameters at each time point t_k were decoded from a set of data points, containing the respective as well as six prior time points of EEG data $\{t_{k-6}, t_{k-5}, \ldots, t_{k-0}\}$ in each electrode (55 remaining channels after removal of the AF row), sampled at 20 Hz. As a result, a total of $7 \times 55 = 385$ temporal features were used to decode the movement parameters (position x, position y, velocity x, velocity y) at one single time point t_k. After windowing the data of the four calibration snakeruns (48 trials, 23 s each) according to this feature structure, the motor decoding was performed using a combination of PLS regression and consecutive smoothing via an UKF (Martínez-Cagigal *et al* 2020).

2.7. Analysis

2.7.1. Sensor space

Pearson's correlation coefficient r was used as a quantitative evaluation metric for the participant's performance levels in sensor space. As the decoder model had to be fit anew with each session, inter-session variances (varying impedance, slightly different electrode positions etc) were removed by normalizing the correlations from the online trials (50% and 100% EEG feedback) with the mean correlation achieved during the offline calibration snakeruns of the respective session. For both paradigms, the chance levels were calculated using a shuffling approach as in (Mondini *et al* 2020). Specifically, EEG data and corresponding snake trajectories from calibration were randomly interchanged for each session to break all causal relations, and a new PLS model was fitted on the shuffled data for 100 times. The chance level of each session and movement parameter was then determined as the 95th percentile of the absolute values of the chance correlations. Significant differences in the respective movement parameters between mean correlations and corresponding chance levels and between mean correlations of two distinct sessions (1↔2, 1↔3, 2↔3) in the respective movement parameters were checked using Wilcoxon's signed rank test. We corrected for multiple comparisons in a total of $n = 30$ tests (four movement parameters $\times$ 3 sessions $\times$ 2 conditions (50/100% EEG feedback snakeruns) + 2 movement parameters $\times$ 3 sessions $\times$ 1 condition (freeruns)) by adjusting the significance level ($\alpha = 0.05$) using the false discovery rate (FDR). Offline analysis on the data was conducted using MATLAB and EEGLAB (Delorme and Makeig 2004).

To overcome the limitations of Pearson's correlation coefficient in analyzing the actual deviation between ground truth and decoded signal (Spuler *et al* 2015), the normalized root mean square error (NRMSE) was consulted. For the normalization of the root mean square error, the side length of the smallest square containing all depicted snake trajectories (960px) has been used. Additionally, to gain insights on the scale of the decoded signals, the amplitude ratio was calculated as the ratio between the variance of the decoded and the variance of the depicted signal.

2.7.1.1. Snakeruns

For the online snakeruns, the normalized correlations in all movement parameters between snake position and EEG-decoded trajectory during each single trial were calculated for each participant and session. The average correlation per session was then grand averaged across all participants for both feedback conditions.

2.7.1.2. Freeruns

Because no dynamic information was depicted on screen during the freeruns, a time series as a ground truth to measure the correlation of the decoded trajectories against was missing in this paradigm. As a replacement, the target position on screen was inferred via horizontal and vertical bipolar derivations of blink-cleaned, low-pass filtered (3 Hz) and downsampled (20 Hz) EOG data. Specifically, for the horizontal component, the difference between the signals at the outer canthi of both eyes was calculated and the correlation with the EEG-decoded position x coordinate was determined. For the vertical component, the signal difference between the EOG electrodes above and below the left eye was determined and the correlation with the EEG-decoded position y component was calculated.

2.7.2. Source space

In addition to the detailed analysis of the decoding performance in sensor space, a general analysis of the decoding performance over sessions was gained by investigating the decoder itself on the source level. As mentioned before, PLS regression was used to find a connection between our selected features $X \in \mathbb{R}^{T\times 385}$ (i.e., the windowed processed EEG data) and target variables $Y \in \mathbb{R}^{T\times 4}$ (i.e., the directional movement parameters from the snake) in T time points. As described in (Mondini *et al* 2020, Kobler *et al* 2020a), this connection is found in the form of a weight matrix $W \in \mathbb{R}^{385\times 4}$ fulfilling $Y = XW$. This corresponds to a backward model, in which W is functioning as a filter applying weights to the features according to their importance. However, to identify the neural correlate to each of the target movement parameters within the PLS model, the respective forward model, i.e. the activation pattern $A = \mathrm{Cov}(X)\, W \mathrm{Cov}(Y)$, is required for meaningful interpretation (Haufe *et al* 2014).

For this reason, we calculated the activation patterns corresponding to the online decoder model for each movement parameter, participant, and session. Because of inter-participant variations in the amplitude of these activation patterns, we normalized

the patterns of each participant with respect to the mean global field power (GFP) across the patterns corresponding to the 100 offline chance permutations that were used before for the chance level estimation of the correlations in sensor space (cf section 2.7.1). Specifically, we calculated the activation pattern to each of the chance models, evaluated its standard deviation across all electrode channels at lag zero, and finally took the mean across all models to find the GFP to all four movement parameters as done in (Mondini *et al* 2020). Data analysis was performed with Brainstorm (Tadel *et al* 2011). Within Brainstorm, we used OpenMEEG (Gramfort *et al* 2010) to generate head models for each participant and session. We co-registered the ICBM152 boundary element model (BEM) (Kybic *et al* 2006) to the electrode positions that we recorded prior to each session (ELPOS, Zebris Medical Gmbh, Germany) using nasion and preauricular points as anatomical landmarks. To control for deviations between each participant's head topology and the BEM, the electrode positions were projected onto the template head model's surface. For the conductivities within each of the three layers of the BEM model (cortex, skull, scalp), we adjusted the default value to (1, 0.008, 1) as in (Mondini *et al* 2020, Kobler *et al* 2020a). Eyerun data of each session, functioning as resting state data, were cleaned of eye artifacts (Mondini *et al* 2020, Kobler *et al* 2020b), freed of the AF channel row, re-referenced to the common average reference and finally cleaned of electrode pops and drifts (Kobler *et al* 2019, Mondini *et al* 2020, Kobler *et al* 2020b) to calculate the noise covariance matrix needed for generating the head model in OpenMEEG. The corresponding inverse solution was found via minimum norm imaging, using sLORETA (Pascual-Marqui 2002) to calculate the current density map. No limitations on the dipole orientations were set, yielding three elemental (Cartesian) dipoles in $n = 15.000$ vertices. These 3 n data points were then flattened by taking the Euclidean norm of the elemental dipoles in each voxel.

To estimate a baseline (chance level) activation pattern for each of the normalized movement parameter patterns generated in this fashion, the patterns corresponding to the 100 chance permutation models generated earlier to estimate the GFP were averaged in source space for each movement parameter, participant, and session. Next, we calculated the difference between the decoder pattern of the movement parameters in the online model and their respective averaged baseline activation pattern. These difference patterns were then averaged across participants for each movement parameter and session. For further analysis, the difference patterns of all movement parameters were each projected onto an atlas of 20 regions of interest (ROI) by taking the mean activation across all voxels per ROI. Taking into account previous works (Mondini *et al* 2020, Kobler *et al* 2020c), the ROI were defined as superior frontal gyrus (SFG), pre- and postcentral gyri (PrG, PoG), superior and inferior parietal lobules (SPL, IPL), occipital gyrus (OcG), paracentral lobule (PCL), precuneus and cuneus (PCun, Cun) and lingual gyrus on both hemispheres, adapted from the Desikan-Killiany atlas (Desikan *et al* 2006). The respective difference distributions across all participants for each movement parameter, ROI and session were then calculated and plotted.

In addition to the investigation of differences between decoder pattern and baseline activation pattern, a non-parametric permutation paired t-test (Nichols and Holmes 2002, Maris and Oostenveld 2007) was consulted to check for significant activity differences between the decoder patterns of the respective sessions, resulting in three pairwise comparisons (session $1 \rightarrow 2$, $1 \rightarrow 3$, $2 \rightarrow 3$) in the previously defined ROI. For 4 movement parameters, 7 time lags, 20 ROI and 3 comparisons, the total number of tests amounted to 1680. We accounted for these multiple comparisons using FDR to adjust the p-values at 0.05 significance level (Benjamini and Hochberg 1995, Yekutieli and Benjamini 1999).

2.8. Participant with SCI

To investigate the feasibility of attempted movement decoding in potential end users, we invited a participant (male, 35) with a cervical spinal cord lesion for two measurements.

The participant received a traumatic complete (AIS A, (Maynard *et al* 1997)) SCI at neurological level of injury C2 in 2003 due to a motorbike accident. He is artificially ventilated (mobile device) and can only move his eyes and face and generate very little head movements. He has no sensory impression below level C2 (neck downwards). For two measurements he was traveling to the lab in Graz for approximately one hour per direction, which he was compensated for.

On both occasions, the participant with SCI was faced with the identical paradigms and feedback conditions presented to the able-bodied participants as well (offline calibration, 50% and 100% EEG feedback snakeruns, and freeruns), however with two instead of three runs each for 50% and 100% EEG feedback snakeruns and freeruns in the online part to shorten measurement time (see adjusted measurement pipeline, figure 1(e)). In the first measurement, we assessed the feasible decoding performance in an *observation* condition (Kobler *et al* 2020c); specifically, the participant with SCI was asked to complete the tracking and tracing tasks solely visually and without attempting movement. During the second measurement, in the *attempted movement* condition, the same tasks were completed again, finally with the same instructions as non-disabled participants by involving attempted movement of his formerly dominant right arm.

In terms of offline analysis, for the sensor space, the exact same procedures were conducted for both able-bodied participants and the participant with SCI (cf section 2.7.1). Likewise, the processing in source space largely coincided (cf section 2.7.2), with the only exception being the data used for the noise covariance matrix to calculate the head model. Due to noisy eyerun data of the participant with SCI recorded during session 2, the eye artifact attenuation model of session 1 was used offline to generate an additional offline decoder model for analysis, which was then evaluated instead of the online model generated for online feedback during the measurement. Additionally, as eyerun data were also used to calculate the noise covariance matrix for the head model in source space for the able-bodied participants, data of the breaks between the single calibration snakerun trials (4 s each) had to be used for the participant with SCI instead. To ensure comparability between both sessions of the participant with SCI, calibration snakerun break data were used to infer the noise covariance matrix for session 1 as well.

3. Results

3.1. Sensor space analysis

3.1.1. Online snakeruns (50%–100% EEG feedback)

The normalized grand average correlations between snake and EEG-decoded trajectories in each directional movement parameter (position *x*, position *y*, velocity *x*, velocity *y*) and session are shown both for the 50% EEG feedback condition (figure 2(a)) and the 100% EEG feedback condition (figure 2(b)). Grand average correlations for each parameter, session and feedback condition are observed significantly ($\alpha = 0.05$) above chance level at approximately 0.4–0.5r_c, with r_c denoting the mean correlation achieved during the calibration snakeruns of the respective session (table S2, supplementary material). Notably, all single participant means (black dots), ranging between 0.5–1.5r_c, are found above chance level already, except for position *y* during the 100% EEG feedback snakeruns of session 1.

For quantitative evaluation of the decoding performance without normalization to the mean correlation achieved in the calibration runs of each respective session, median raw correlations can be found in figure S3 (supplementary material); exemplary snake trajectories and corresponding decoded trajectories for participant P9, session 2, are shown in figure S4 (supplementary material). The NRMSE and amplitude ratios across all participants for calibration and online snakeruns can be found in table 1. Regarding both grand average NRMSE, as well as grand average amplitude ratio, a worsening with increasing percentual importance of the EEG for decoding can be observed. While the NRMSE stays largely unaffected (increase from on average 10% to on average 12% of the used TV screen range from calibration to 100% percent EEG feedback snakeruns over all sessions), the amplitude ratio worsens noticeably in terms of both grand average and standard deviation. However, for these metrics as well, session 2 yields the best results over all paradigms regarding grand average and standard deviation.

In terms of decoding performance, significant improvement over sessions was only found from session 1 to session 2 during the 100% EEG feedback condition in the position *x* parameter. However, the 50% EEG feedback condition nonetheless exhibits a notable increase in grand average correlations in each movement parameter from session 1 to session 2, followed by a consecutive performance degradation from session 2 to session 3. A similar trend can be observed regarding the movement parameters in the *x* coordinate in the 100% EEG feedback condition, though decoding performance in the movement parameters in the *y* coordinate is found to steadily decrease across sessions in this condition. Additionally, a general decrease in decoding performance with respect to the mean calibration correlation can be observed from the 50% to the 100% EEG feedback condition.

When investigating the normalized single participant correlation means, an increase in performance can be observed for approximately half of the ten participants (P1, P3, P7, P8–10) from session 1 to any later session in most movement parameters and feedback conditions (see figure 3). Additionally, we noted a personal affinity towards a preferred decoding direction (see figure 3); in most participants (P1, P4–6, P8–10), a clear performance gap is visible between the two coordinates. This effect is not observed in the grand average (figure 2).

3.1.2. Freeruns

For the freeruns, the normalized grand average correlations between EOG-inferred and EEG-decoded trajectories were evaluated, as shown in figure 2(c). Single participant means, ranging from 0.5 to 1.5rc, are observed strictly above chance level in all parameters and sessions. Wilcoxon's signed rank test revealed significant differences between grand averages and corresponding chance levels in all sessions for both movement parameters.

As can be seen, lower correlations are observed in the freeruns compared to the snakeruns completed prior. Additionally, no significant changes in decoding performance from session to session were observed. However, a similar increase in performance from session 1 to session 2 with a consecutive degradation from session 2 to session 3 as seen in the snakeruns is seen in position *x*.

3.2. Source space analysis

Apart from analyzing the correlations of our decoded trajectories with a given ground truth in sensor space, we also investigated the intrinsic decoder properties

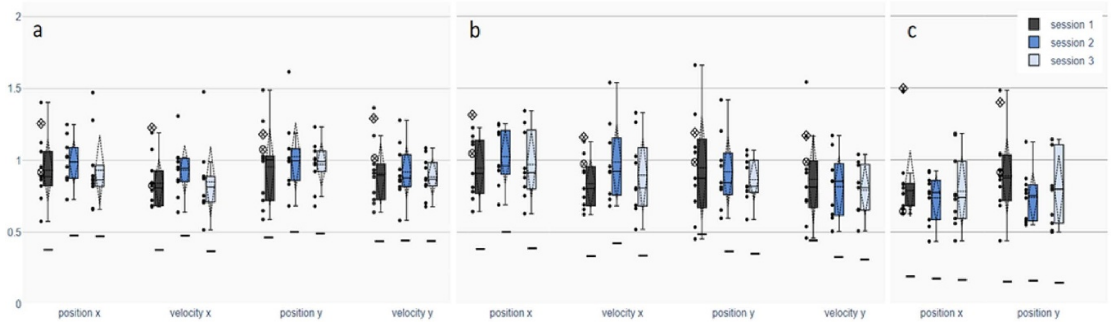

Figure 2. Normalized correlations per movement parameter over sessions, online snakeruns and freeruns. Grand average normalized correlations (dashed vertical lines) between depicted snake trajectory or EOG-inferred trajectory, respectively, and EEG-decoded trajectory with standard deviations (dashed tails), median and 25th/75th percentiles (boxes), single participant means (black dots) and median chance levels (horizontal solid lines below) for all movement parameters and sessions for (a) 50% EEG feedback snakeruns, (b) 100% EEG feedback snakeruns and (c) freeruns. All data were normalized with respect to the mean calibration correlation (r_c) of each respective session. For all prerequisites, mean correlations are observed significantly above chance level at approx. 0.4–0.5r_c. Crosshair diamond and circle correspond to *observation* and *attempted movement* performance of the participant with SCI.

Table 1. Normalized root mean square error (NRMSE) and amplitude ratio. Grand average (GA) NRMSE and amplitude ratio with respective standard deviation (STD) between decoded and depicted trajectories for calibration and online snakeruns in all sessions, averaged over all movement parameters.

	NRMSE (GA + STD)			Amplitude ratio (GA + STD)		
Paradigm	Session 1	Session 2	Session 3	Session 1	Session 2	Session 3
Calibration	0.10 (0.01)	0.10 (0.01)	0.10 (0.01)	1.01 (0.05)	1.01 (0.04)	1.01 (0.04)
50% EEG feedback snakeruns	0.11 (0.01)	0.11 (0.01)	0.12 (0.01)	1.08 (0.17)	1.07 (0.11)	1.07 (0.14)
100% EEG feedback snakeruns	0.13 (0.02)	0.11 (0.01)	0.12 (0.02)	1.15 (0.27)	1.04 (0.14)	1.09 (0.27)

over sessions in source space. The grand average activity difference per voxel between decoder activation patterns and respective baseline activation patterns for each movement parameter and session at time lag 0 is shown in figure 4(a).

Across the ten participants, we observed that these grand average difference patterns become more distinct over sessions. Specifically, the activated sector in the parieto-occipital region for the movement parameter velocity *y* steadily increases in size across sessions, reaching up until the central region in session 3. Similar increases in size of the activated regions are also observed for position *x*, with increases from occipital to parieto-occipital regions, and velocity *x*, with increasing activation in the posterior parietal cortex, from session 1 to session 2.

After downsampling to our predefined atlas of 20 ROI (figure 4(c)), no significant differences between decoder patterns and baseline activation patterns were found in any movement parameter, session, and ROI for any of the seven time lags. The resulting difference distribution across the single participant differences per movement parameter, ROI, and session (lines), as well as the respective grand average (dots) are shown in figure 4(b). As can be seen, the grand average values increase over sessions in most movement parameter and ROI combinations, with session 2 or session 3 yielding the most distinct differences between decoder and baseline pattern in approximately 85% of the cases. In about 90% of the cases, an average increase in difference from session 1 to any later sessions is observed, of which 65% correspond to a maximum difference seen during session 2.

In terms of ROI, irrespective of the movement parameter, the highest activation (positive sign) compared to baseline (figure 4(b)) is observed in the parieto-occipital regions. For position *x*, all regions apart from SFG, PrG and PoG are engaged in each session, with the highest activations seen in the contralateral hemisphere. In contrast, only the contralateral IPL shows activation throughout all sessions in movement parameter position *y*, coinciding with its largely erratic difference patterns (figure 4(a)). Both velocity parameters exhibit clear engagement of central through occipital regions, with disengagement only seen in the SFG in velocity *x* and velocity *y*, and in the PrG in velocity *y*. The highest activations in the velocity parameters are observed in the contralateral SPL, PCL, PCun and Cun areas. In general, the velocity parameters show more consistency than the positional parameters (see figure 4(a)) due to the irregular pattern seen in position *y*.

Regarding the behavior of the difference patterns across sessions, likewise to the comparison between decoder patterns and baseline activation patterns, no significant differences can be reported for any

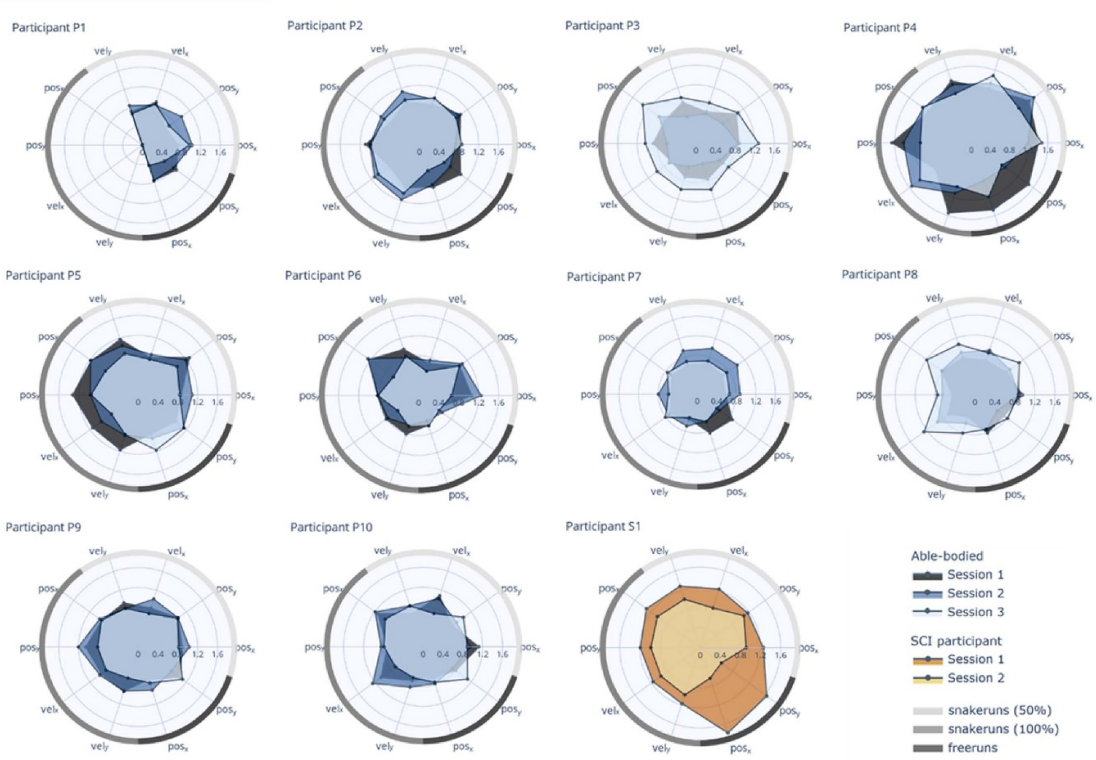

Figure 3. Normalized single participant correlation means across sessions, online runs. Normalized correlation means for each able-bodied participant (blue shades) across all respective trials in 50% (light gray section) and 100% (medium gray section) EEG feedback snakeruns and freeruns (dark gray section) over the three sessions (dark to light blue). For participant P1, 100% EEG feedback snakerun data were not recorded. Equal information is plotted for the spinal cord injured participant S1 (brown shades) during the *observation* (session 1) and the *attempted movement* (session 2) tasks (dark to light brown).

pairwise comparison (session 1→2, 1→3, 2→3) in any movement parameter, ROI, and time lag.

3.3. Participant with SCI

Following our study on learning effects confirming the feasibility of decoding from attempted movement in able-bodied participants, we conducted two consecutive measurements involving a participant with SCI to assess the decoding performance in potential end users. The participant's performance levels in two separate measurements, evaluated in sensor space, are shown as diamond (observation) and circle (attempted movement) in session 1 of figure 2. Because these measurements involved two different conditions (observation in session 1, attempted movement in session 2, see section 2.8), a comparison was only possible with results of session 1 in the able-bodied participants. As can be seen, the disabled participant's correlations during observation in both the snakeruns and the freeruns are on par with top-performing participants of the able-bodied attempted movement group, with even the best performance in 40% of the cases. As such, the decoding performance in the participant with SCI was found well above chance level. In contrast to the observation condition, however, a notable decrease in correlations is shown during the disabled participant's attempted movement measurement. The performance of the participant with SCI dropped to average at best, lowest of all participants in the worst case, though still well above chance level.

As with the able-bodied participants, the SCI participant's decoder activation pattern was investigated in source space as well (figure 5). The difference patterns between decoder pattern and baseline activation pattern for each movement parameter at lag 0 in the observation and the attempted movement condition are shown in figures 5(a) and (b). Here, dark red color implies regions of higher, dark blue color regions of lower activation than baseline activation. While clear engagement of parieto-occipital regions is present in position x and velocity x during attempted movement, the patterns concerning observation do not appear as distinct, also involving frontal activation mostly observed in the contralateral hemisphere. For both conditions, the difference patterns of position y show parieto-occipital activation, though the activity appears attenuated during attempted movement. The difference between both conditions is shown in figure 5(c)., with bright red color corresponding to regions of higher, bright blue color corresponding to regions of lower activation during attempted movement compared to observation. For both parameters in the x coordinate, additional activation is seen in the parieto-occipital regions during attempted movement, with weak activation also shown across

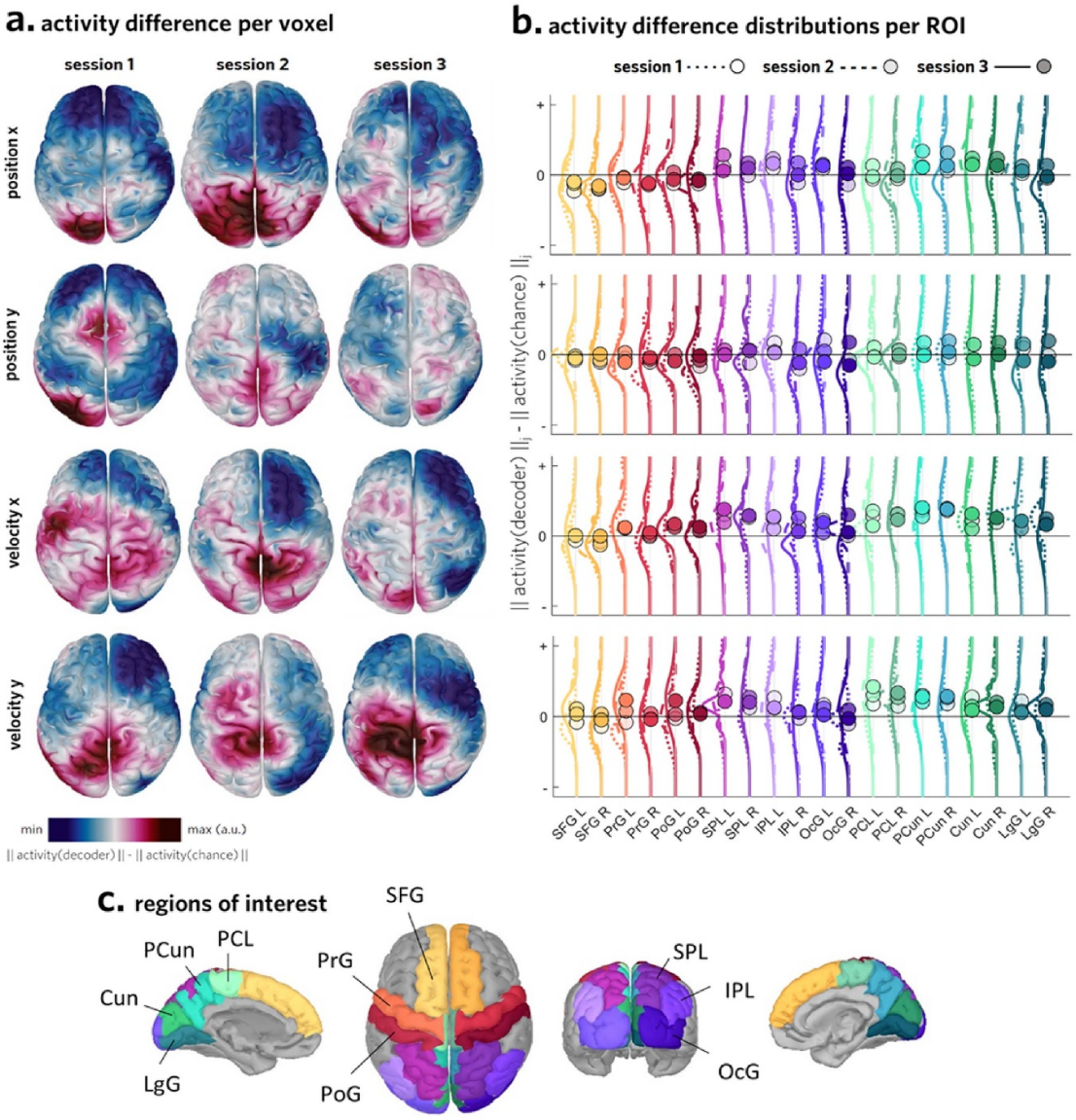

Figure 4. Activity over sessions in source space. (a) Grand average difference activity per voxel between decoder model activation pattern and baseline activation pattern in source space at lag 0 for all movement parameters. Red color indicates regions of higher (activation), blue color indicates regions of lower activation than baseline (deactivation). (b) Density estimates and corresponding grand averages of the activity difference across all participants per session, ROI, and movement parameter. (c) Cortical representation of the 20 predefined regions of interest (ROI) comprising superior frontal gyrus (SFG), pre- and postcentral gyri (PrG, PoG), superior and inferior parietal lobules (SPL, IPL), occipital gyrus (OcG), paracentral lobule (PCL), precuneus and cuneus (PCun, Cun) and lingual gyrus (LgG) on both hemispheres.

the contralateral central regions (PoG, PrG) corresponding to the sensorimotor areas in the positional parameter. For the velocity *y* parameter, the highest intensity of the difference in activation of both sessions is seen in the contralateral central and parietal regions (PoG, SPL).

4. Discussion

Cervical SCI or degenerative diseases leading to limited motor function necessitate the restoration of upper limb movement by means of natural, continuous movement decoding to control a man-made end effector (e.g. neuroprosthesis, robotic arm). Our group recently reported better than random and continuous decoding of movement information from EEG signals (Martínez-Cagigal *et al* 2020, Mondini *et al* 2020, Kobler *et al* 2020c). However, taking into consideration the actual target group for these types of BCIs, i.e. people experiencing severe limitations in motoric function, calibrating the decoder with executed movement is not an option.

In this study, we therefore addressed two issues: first, making the BCI accessible also for persons with motor disabilities, and second, investigating changes in the corresponding decoding performance over time. To cater the decoder also to motor-impaired BCI end users, we changed the setup from executed movement to attempted movement (Ofner *et al* 2019,

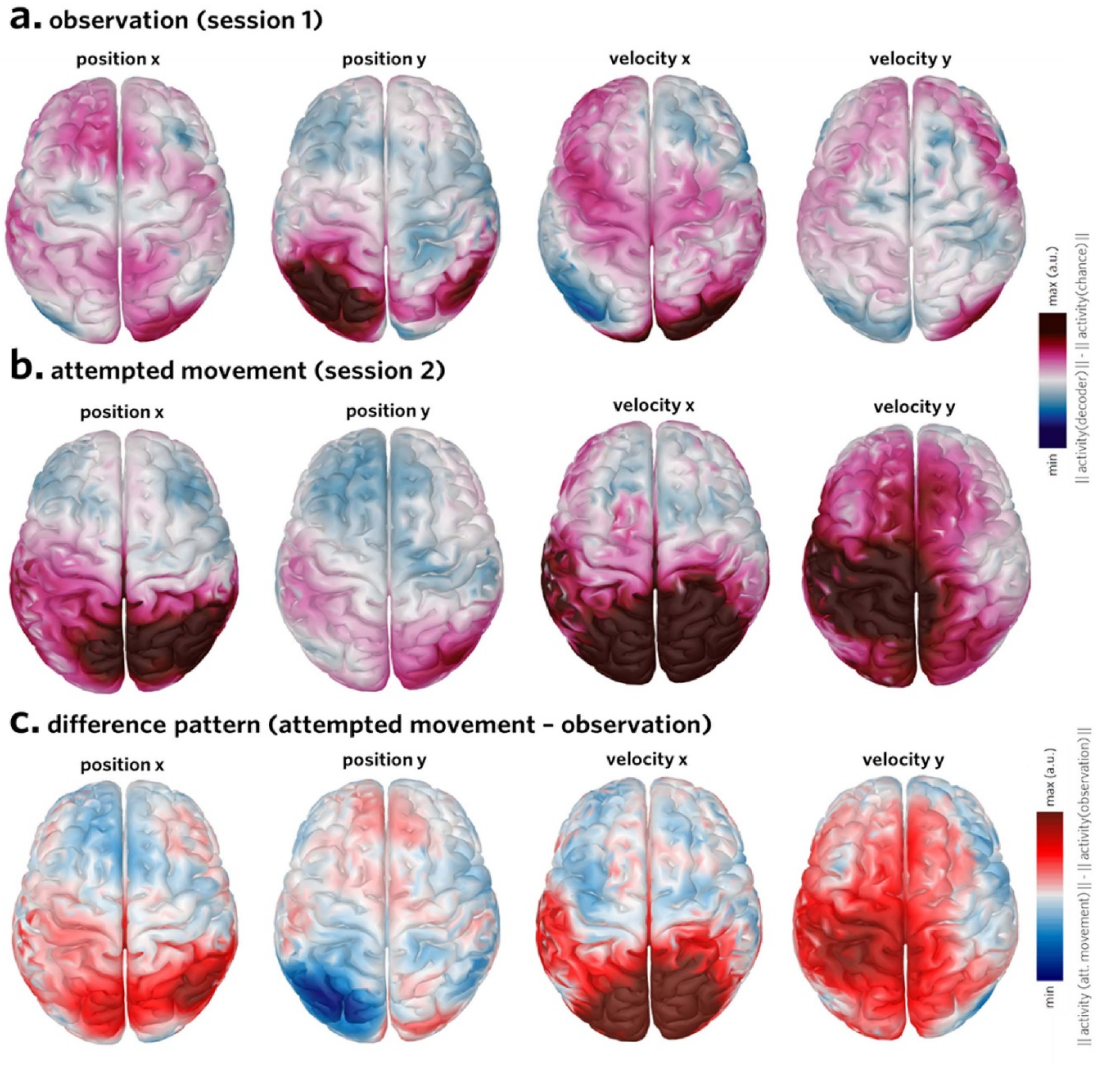

Figure 5. Activity in source space, spinal cord injured participant. Difference patterns between decoder model activation pattern and baseline activation pattern during (a) session 1 (*observation*) and (b) session 2 (*attempted movement*) in the spinal cord injured participant. Red color indicates regions of activation, blue color indicates regions deactivation compared to baseline. (c) Difference patterns between (a) and (b); bright red color indicates activation; bright blue color indicates deactivation during *attempted movement* compared to *observation*. The difference patterns for all movement parameters are shown at lag 0.

Müller-Putz *et al* 2021, Pulferer *et al* 2021). As a means of dealing with the anticipated decline in decoding performance compared to executed movement decoding, driven by less engagement of the motor areas during attempted movement, we further investigated the effect of the users themselves on the BCI. Over three sessions, we monitored the respective decoding performance of ten able-bodied participants during attempted movement with the hypothesis that improvements may be facilitated by employing task-specific user training. Our findings can be summarized to three central results.

First, the decoding of attempted movement in able-bodied participants is possible significantly above chance as was seen for executed movement before (Martínez-Cagigal *et al* 2020, Mondini *et al* 2020, Kobler *et al* 2020c). Second, depending on the personal approach to the task respectively the individual level of motivation of the participants, approximately half of the participants experienced increases in performance over multiple sessions, which however were not found to be statistically significant. Increasingly distinct decoder patterns seen in source space suggest that user training can play a role in continuous motor decoding. However, the lack of a significant difference in patterns over sessions rather promotes the use of generalized decoding models utilizing source space information, as the decoding patterns, from a statistical point of view, appear to remain stable over sessions. And third, decoding attempted movement continuously and non-invasively is possible above chance level not only in able-bodied participants, but in persons with SCI as well. Though sensor space analysis suggests decreasing decoding performance with the additional mental strain of attempting movement, distinct differences in decoder patterns compared to the observation condition imply the potential importance of movement

information for decoding in source space, even in participants who have not engaged their motor areas for years.

4.1. Sensor space

Within this study, we report correlations well above chance level for continuous decoding not only from executed movement, but from attempted movement as well, suggesting attempted movement as a possibility to close the gap from non-disabled to motor-impaired end users. For all feedback conditions (50% and 100% EEG feedback), movement parameters (position x, position y, velocity x, velocity y) and sessions (1–3), grand average correlations across all participants significantly above chance level were observed. During the target tracking tasks (50% and 100% EEG feedback online snakeruns), we obtained grand average correlations in sensor space across all movement parameters of 0.31 (0.02 SD), 0.32 (0.02 SD), and 0.30 (0.02 SD) for sessions 1–3. In terms of a general assessment of the decoding performance related to attempted movement tasks, and considering the standard deviations, this ranges between the grand average correlations of 0.40 (0.06 SD) during executed movement and 0.31 (0.08 SD) during observation described by (Kobler *et al* 2020c) for a similar target tracking task of shorter duration (16 s), likewise using the PLS UKF decoder. These findings confirm our hypothesis of decreasing decoding performance from executed movement to attempted movement, until the lowest performance is reached during an observation only task, resulting from declining engagement of the motor areas from actual movement to a strictly visual task. While we did observe a trend combining an increase in decoding performance from session 1 to session 2 with a consecutive degradation from session 2 to session 3 in the average correlations during the tracking tasks (figure 2), as well as within approximately half of the single participant means (figure 3), the existence of a learning effect has not convincingly been found over the limited amount of three sessions. As no questionnaires were offered in this study, a quantitative analysis of the respective motivation and engagement of each participant over sessions as an influence for the mentioned trend is missing. However, participants generally felt motivated and assertive during the first two sessions; the mismatch in expectations and actual improvements and a varying personal frustration tolerance may have led to a drop in performance during the third session in most participants.

When investigating the general decoding performance, favored decoding directions varying across participants were observed. Approximately two thirds of the participants (figure 3, P1, P3, P7-10) showed clear differences in decoding performance between x and y coordinates. As the exact same calibration snakeruns were shown in the same order in each session and in fact not randomized, this effect cannot be attributed to different conditions during data acquisition for fitting the decoder. Additionally, the trend towards a preferred coordinate is not observed in the grand average, confirming the assumption that this effect is introduced by the participants themselves.

One of the main challenges concerning this study, namely the generally high variances in decoding performance from session to session as well as the inter-participant variance, was addressed by normalizing all correlation data with respect to the mean correlation achieved during the calibration runs of the corresponding session. Taking this normalization into account, a decrease in decoding performance can be observed from the 50% to the 100% EEG feedback condition (figure 2. Grand averages move farther below $1 \mathrel{\hat{=}} \mathrm{rc}$ over the course of the paradigms/-conditions), which may be explained threefold. First, going from a mixture of snake and EEG-decoded trajectory (50%) to a solely EEG-decoded trajectory (100%) inherently worsens the decoding performance. Second, the more time passes between calibration runs and online decoding, the more the performance diminishes. As the sequence during the online part comprised three 50% EEG feedback snakeruns, then three 100% EEG feedback snakeruns, and finally the 100% EEG feedback freeruns, a decline in correlations in this order is to be expected. And third, individual motivation and engagement of each participant vastly influence any BCI operation. With the long measurement times (3–4 h), the inhomogeneity of feedback conditions, as well as the monotony of the tasks, may have led to fatigue and weariness, further depressing the decoding performance over time during as well as across sessions.

In the freeruns, a further performance drop compared to the snakeruns was observed. As with the snakeruns, this may be explained in part by the increasing time span from calibration, in part by the exclusively EEG-decoded trajectories that were used in this paradigm. However, the lack of the snake as a ground truth during the freeruns required the EOG-inferred trajectories as a measure, which, compared to the snake, trivially introduced more uncertainties in the evaluation. Nonetheless, the spread of the single participant means remained comparable with the spread observed for the snakeruns, and grand average correlations significantly above chance level were observed also for the freeruns. In general, the self-paced nature of the freerun (tracing) task was perceived as more difficult.

4.2. Source space

Though a permutation paired t-test, corrected for multiple comparisons, showed no significant difference between decoder and baseline patterns, distinct regions of activation and deactivation for the decoding of the respective movement parameters became visible in the grand average difference between decoder activation pattern and baseline activation

pattern (figure 4(a)). For all parameters, except position *y*, the grand average difference patterns largely retained their qualitative appearance across sessions, meaning no drastic changes were observed, and the cortical origins for the decoding of each movement parameter tended to remain stable, which might be utilized in transfer learning approaches based on source space decoding. In the case of position *y*, the patterns changed noticeably over sessions. Most likely, the cause of this effect lies in the measurement setup itself; as the participants' dominant arm was strapped to the armrest, movement in *y* direction (corresponding to height on screen) could not be understood in a straightforward way, unlike the left and right movements corresponding to the *x* coordinate. As the participants were instructed to attempt arm movement as if wielding a computer mouse, moving the feedback dot upwards on screen corresponded to a forward motion of the strapped limb. This counterintuitive translation between movement and perception may have led to a strong variation in decoder patterns across participants and therefore diffuse grand average patterns. The activity difference distributions (figure 4(b)) in position *y*, strongly centered around zero without a clear trend regarding importance of ROI across sessions, confirm this assumption.

In the remaining parameters (position *x*, velocity *x*, velocity *y*), mostly the parieto-occipital regions were engaged, with additional importance of the central regions above PrG and PoG in the velocity parameters. All three parameters share a high bilateral focus of decoding importance in the PCun (BA 7), which goes in agreement with findings of prior studies from our group (Mondini *et al* 2020, Kobler *et al* 2020c). From macaque studies, the PCun region was found to share a connection with both the sensorimotor region as well as the visual cortex (Margulies *et al* 2009). Precisely, its importance in shifting attention between different visual inputs—as required in dividing one's attention between snake and feedback dot in our experiment—is described in (Wenderoth *et al* 2005) and stands in agreement with our findings. Further, the session-to-session variation in activation of this area may also be related to the user's adaptation to the BCI. Additionally, it has since been known that the posterior parietal cortex (PPC) is tightly involved in visuospatial perception, specifically, in defining and commanding movement goals in intrinsic visual coordinates (Fernandez-Ruiz *et al* 2007, Lindner *et al* 2010). Moving incrementally through the mental workload processed in the PPC induced by the tracking task, the visual information shown on screen would first need to be assessed in terms of priority (parietal eye field, PEF) (Medendorp *et al* 2011), next in terms of movement direction and speed (middle temporal visual area, V5) (Born and Bradley 2005), and finally, a clear reaching/pointing decision has to be made (V6A resp. parietal reach region, PRR) (Pitzalis *et al* 2013, 2015, Christopoulos *et al* 2015). In our analysis (figure 4), activations above all regions are seen, corresponding to contralateral engagement of SPL, IPL as well as parts of the OcG.

In terms of a learning effect over sessions, activity difference patterns (figure 4(a)) and activity difference distributions across all participants (figure 4(b)) qualitatively hint at the possible existence of a learning effect induced by BCI user training. An increase in average difference (decoder—baseline) from session 1 to any later session was seen in 90% of the conditions (4 parameters $\times$ 20 ROI). Specifically, 65% of these improvements were observed during session 2, confirming the results obtained by the correlation analysis conducted in sensor space. Comparing the difference patterns (figure 4(a)) of session 1 and session 2 in the movement parameters position *x*, velocity *x* and velocity *y*, a trend to larger activations in the SPL and IPL, as well as additional activation in the central areas (PrG and PoG, PCL) can be observed. These regions were reported as relevant to motor skill learning during a goal-directed, center-out movement task (Bédard and Sanes 2014). Additionally, engagement of the bilateral IPLs during motor skill learning was reviewed in (Seidler *et al* 2012), coinciding with our observations. However, statistical tests revealed no significant differences in the source space as well. As the limited number of sessions prevents definite judgment on the presence of a learning effect, the dimension of performance improvement via user learning remains to be seen. At this point, the non-significant changes in decoder patterns over sessions may rather promote decoding methods utilizing source space information for the development of generalized classifiers.

4.3. Participant with SCI

In the participant with SCI, ambiguous results have been found. On the one hand, the evaluation in sensor space yielded top performance of the participant with SCI in four of all ten movement parameters comprising snakeruns and freeruns during the observation task (figure 2), with a general performance level on par with top-performing able-bodied participants during attempted movement (figure 2, cross-haired diamonds). This may be explained by an indisputable superiority of the participant with SCI over the able-bodied participants regarding the level of attention during observation and the necessity to rely on exact eye movement while being not able to turn his head, resulting from years of living with severe limitations in motor function. In contrast to this, a clear decrease in performance in sensor space was seen during the attempted movement task (figure 2, cross-haired circles). This confronts initial assumptions, based on the results of the able-bodied participants, that any additional information stemming from the

motor areas—as would be expected when switching from a strictly observing condition to movement attempts—would contribute constructively to the decoding performance regarding continuous movement tasks. Indeed, during simple classification tasks based on event-related desynchronization/synchronization in participants with SCI close to reaching chronic state, it has been demonstrated that the additional information during attempted movement compared to simple MI may lead to increasing classification accuracies (López-Larraz *et al* 2012). A recent study further confirmed significantly increased accuracies in discriminating MAs from a resting condition when compared to MI (Chen *et al* 2021). Compared to these results, the continuous decoding performance we have observed within this study in the disabled participant, whose trauma dates back to 2003, worsened considerably compared to the observation task, most likely explained by the additional mental strain introduced by the attempt to engage areas that have not been employed in years.

Regarding the source space analysis conducted on the data of both sessions, during attempted movement (figure 5(b)), similar patterns to the grand average of the able-bodied participants are observed (figure 4(a)), whereas the patterns during observation (figure 5(a)) exhibit no clear structure. In the difference patterns (figure 5(c)), the additional activation during attempted movement compared to observation is depicted, indicating clear additional engagement of the parieto-occipital areas in most of the movement parameters. As such, even though the results in sensor space indicate the contrary, decoding in source space may benefit considerably from the additional information above the motor areas compared to a strictly visual task.

Disregarding the ambivalent results in sensor and source space in the sessions conducted with the participant with SCI, correlations well above chance level have been found for either task (figure 2). Compared to prior studies, already commending attempted movement employed in cue-based classification tasks in participants with SCI (Ofner *et al* 2019, Chen *et al* 2021), we were able to confirm that decoding continuously (non-cue-based, trial duration 23 s) and non-invasively from attempted movement is also feasible in persons with severe limitations in motoric abilities. This affirms attempted movement as a possible link connecting studies in able-bodied participants with studies involving actual end users.

5. Limitations

The central limitations of this study may be summarized to two major challenges, being first paradigm-related and second user-related issues.

Long measurement times due to the extensive calibration time, different experimental conditions such as variances in the electrode montage, as well as the ambiguous task that was presented, namely the attempted cursor movement involving forward and backward movement that is then translated to upward and downward movement of the cursor on screen, basically prompting an internal coordinate transform in the participants, must be attributed to the former, paradigm-related issues. As a possible solution to the long calibration phase, transfer learning (intra-participant from session to session, or even inter-participant) may be mentioned. Developing a stable decoder needing only a minimum amount of recent data may shorten the measurement times considerably. The inter-session variances have successfully been addressed by normalizing the online performance levels with respect to the mean achieved calibration correlation of the respective session, however, for future works, a different task must be devised to circumvent projecting depth to height information. Additionally, it should be avoided to present more than one paradigm (choosing either snakeruns or freeruns) to deepen any individual progress.

Regarding the latter, user-related problems, two major points should be addressed in further studies. First, the monotony of the task needs to be minimized to avoid triggering frustration and fatigue. This can be achieved by actively involving the user beyond offering visual online feedback, for example via constructing the trials in the form of levels, allowing the users to upgrade or gain merits by improving their performance. And second, the different levels of engagement and motivation in the participants should be monitored carefully. This can be achieved by presenting the users with questionnaires both prior to and after each session and would additionally allow an investigation on how to promote learning on an individual level.

6. Conclusions

Previous non-invasive studies already indicated that attempted movement may provide relevant information during the classification of cue-based tasks in spinal cord injured participants (López-Larraz *et al* 2012, Ofner *et al* 2019, Chen *et al* 2021). Here, combining the results of two different studies, we report that attempted movement may also be decoded online continuously well above chance level during externally paced target-tracking tasks as well as self-paced tracing tasks (23 s duration per trial), not only in able-bodied participants, but also in a spinal cord injured participant. We observed grand average decoding correlations in sensor space ranging between observed and executed movement, indicating a clear benefit in employing attempted movement over observation tasks to involve participants experiencing severe limitations in motor output. Additionally, we observed a distinguishable though

non-significant difference in decoding performance across sessions in the able-bodied participants, which, eliminating the influence of inter-session variations, may be contributed to a learning effect.

To summarize, our findings in source space, in combination with the results in sensor space, lead to three conclusions: first, the repetition of a visuomotor task may have positive influence on the decoding performance during attempted movement tasks. Second, depending on the monotony of the given task, motivation and engagement of the participants may depress said improvements considerably and should be handled with due caution in future continuous movement studies. And third, and most importantly, continuous decoding of attempted movement is feasible in an online setting well above chance level in both able-bodied and spinal cord injured participants and may thus function as a link between feasibility studies in able-bodied participants to actual applications involving end users

Author contributions

Hannah S Pulferer: conceptualization, formal analysis, writing (original draft, review, editing). Brynja Ásgeirsdóttir: investigation, writing (review, editing). Valeria Mondini: supervision, writing (review, editing). Andreea I Sburlea: writing (review, editing). Gernot R Müller-Putz: conceptualization, supervision, writing (review, editing).

Data availability statement

The data generated and/or analysed during the current study are not publicly available for legal/ethical reasons but are available from the corresponding author on reasonable request.

Acknowledgments

This research was supported by funding from the European Research Council (ERC-CoG 2015 681231 'Feel Your Reach') and NTU-TUG joint PhD program. Supported by TU Graz Open Access Publishing Fund.

ORCID iDs

Hannah S Pulferer https://orcid.org/0000-0002-1956-5322
Valeria Mondini https://orcid.org/0000-0001-7680-6199
Andreea I Sburlea https://orcid.org/0000-0001-6766-3464
Gernot R Müller-Putz https://orcid.org/0000-0002-0087-3720

References

Antelis J M, Montesano L, Ramos-Murguialday A, Birbaumer N and Minguez J 2013 On the usage of linear regression models to reconstruct limb kinematics from low frequency EEG signals *PLoS One* **8** e61976
Bédard P and Sanes J N 2014 Brain representations for acquiring and recalling visual–motor adaptations *NeuroImage* **101** 225–35
Benjamini Y and Hochberg Y 1995 Controlling the false discovery rate: a practical and powerful approach to multiple testing *J. R. Stat. Soc.* **57** 289–300
Black M J *et al* 2003 Connecting brains with machines: the neural control of 2D cursor movement *First Int. IEEE EMBS Conf. on Neural Engineering, 2003. Conf. Proc.* pp 580–3
Born R T and Bradley D C 2005 Structure and function of visual area MT *Annu. Rev. Neurosci.* **28** 157–89
Bradberry T J, Gentili R J and Contreras-Vidal J L 2010 Reconstructing three-dimensional hand movements from noninvasive electroencephalographic signals *J. Neurosci.* **30** 3432–7
Bradberry T J, Gentili R J and Contreras-Vidal J L 2011 Fast attainment of computer cursor control with noninvasively acquired brain signals *J. Neural. Eng.* **8** 036010
Brainard D H 1997 The psychophysics toolbox *Spat. Vis.* **10** 433–6
Charlifue S *et al* 2012 International spinal cord injury quality of life basic data set *Spinal Cord* **50** 672–5
Chen S, Shu X, Wang H, Ding L, Fu J and Jia J 2021 The differences between motor attempt and motor imagery in brain-computer interface accuracy and event-related desynchronization of patients with hemiplegia *Front. Neurorobot.* **15** 706630
Christopoulos V N, Bonaiuto J, Kagan I and Andersen R A 2015 Inactivation of parietal reach region affects reaching but not saccade choices in internally guided decisions *J. Neurosci.* **35** 11719–28
Delorme A and Makeig S 2004 EEGLAB: an open source toolbox for analysis of single-trial EEG dynamics including independent component analysis *J. Neurosci. Methods* **134** 9–21
Desikan R S *et al* 2006 An automated labeling system for subdividing the human cerebral cortex on MRI scans into gyral based regions of interest *NeuroImage* **31** 968–80
Edelman B J, Meng J, Suma D, Zurn C, Nagarajan E, Baxter B S, Cline C C and He B 2019 Noninvasive neuroimaging enhances continuous neural tracking for robotic device control *Sci. Robot.* **4** 31
Fernandez-Ruiz J, Goltz H C, DeSouza J F X, Vilis T and Crawford J D 2007 Human parietal "reach region" primarily encodes intrinsic visual direction, not extrinsic movement direction, in a visual motor dissociation task *Cereb. Cortex* **17** 2283–92
Gramfort A, Papadopoulo T, Olivi E and Clerc M 2010 OpenMEEG: opensource software for quasistatic bioelectromagnetics *Biomed. Eng. Online* **9** 45
Hammer J, Fischer J, Ruescher J, Schulze-Bonhage A, Aertsen A and Ball T 2013 The role of ECoG magnitude and phase in decoding position, velocity, and acceleration during continuous motor behavior *Front. Neurosci.* **7** 200
Haufe S, Meinecke F, Görgen K, Dähne S, Haynes J-D, Blankertz B and Bießmann F 2014 On the interpretation of weight vectors of linear models in multivariate neuroimaging *NeuroImage* **87** 96–110
Hochberg L R *et al* 2012 Reach and grasp by people with tetraplegia using a neurally controlled robotic arm *Nature* **485** 372–5
Kleiner M, Brainard D and Pelli D 2007 ECVP '07 abstracts' *Perception* **36** 1–235
Kobler R J, Kolesnichenko E, Sburlea A I and Müller-Putz G R 2020a Distinct cortical networks for hand movement initiation and directional processing: an EEG study *NeuroImage* **220** 117076

Kobler R J, Sburlea A I, Lopes-Dias C, Schwarz A, Hirata M and Müller-Putz G R 2020b Corneo-retinal-dipole and eyelid-related eye artifacts can be corrected offline and online in electroencephalographic and magnetoencephalographic signals *NeuroImage* **218** 117000

Kobler R J, Sburlea A I, Mondini V, Hirata M and Müller-Putz G R 2020c Distance- and speed-informed kinematics decoding improves M/EEG based upper-limb movement decoder accuracy *J. Neural. Eng.* **17** 056027

Kobler R *et al* 2019 HEAR to remove pops and drifts: the high-variance electrode artifact removal (HEAR) algorithm *Proc. 41th Annual Int. Conf. IEEE Engineering in Medicine and Biology Society (EMBC)* (IEEE Xplore) (https://doi.org/10.1109/EMBC.2019.8857742)

Korik A, Sosnik R, Siddique N and Coyle D 2018 Decoding imagined 3D hand movement trajectories from EEG: evidence to support the use of Mu, Beta, and low Gamma oscillations *Front. Neurosci.* **12** 130

Korik A, Sosnik R, Siddique N and Coyle D 2019 Decoding imagined 3D arm movement trajectories from EEG to control two virtual arms-a pilot study *Front. Neurorobot.* **13** 94

Kybic J, Clerc M, Faugeras O, Keriven R and Papadopoulo T 2006 Generalized head models for MEG/EEG: boundary element method beyond nested volumes *Phys. Med. Biol.* **51** 1333–46

Lindner A, Iyer A, Kagan I and Andersen R A 2010 Human posterior parietal cortex plans where to reach and what to avoid *J. Neurosci.* **30** 11715–25

López-Larraz E *et al* 2012 Continuous decoding of motor attempt and motor imagery from EEG activity in spinal cord injury patients *Annual Int. Conf. IEEE Engineering in Medicine and Biology Society* (available at: www.researchgate.net/profile/Javier-Minguez/publication/235387261_Continuous_decoding_of_motor_attempt_and_motor_imagery_from_EEG_activity_in_spinal_cord_injury_patients/links/00b4952bfed701890f000000/Continuous-decoding-of-motor-attempt-and-motor-imagery-from-EEG-activity-in-spinal-cord-injury-patients.pdf) (https://doi.org/10.1109/EMBC.2012.6346299)

Margulies D S, Vincent J L, Kelly C, Lohmann G, Uddin L Q, Biswal B B, Villringer A, Castellanos F X, Milham M P and Petrides M 2009 Precuneus shares intrinsic functional architecture in humans and monkeys *Proc. Natl Acad. Sci. USA* **106** 20069–74

Maris E and Oostenveld R 2007 Nonparametric statistical testing of EEG- and MEG-data *J. Neurosci. Methods* **164** 177–90

Martínez-Cagigal V, Kobler R J, Mondini V, Hornero R and Muller-Putz G R 2020 Non-linear online low-frequency EEG decoding of arm movements during a pursuit tracking task *2020 42nd Annual Int. Conf. IEEE Engineering in Medicine Biology Society (EMBC)* pp 2981–5

Maynard F M *et al* 1997 International standards for neurological and functional classification of spinal cord injury *Spinal Cord* **35** 266–74

Medendorp W P, Buchholz V N, Van Der Werf J and Leoné F T M 2011 Parietofrontal circuits in goal-oriented behaviour *Eur. J. Neurosci.* **33** 2017–27

Meng J, Zhang S, Bekyo A, Olsoe J, Baxter B and He B 2016 Noninvasive electroencephalogram based control of a robotic arm for reach and grasp tasks *Sci. Rep.* **6** 38565

Mondini V, Kobler R J, Sburlea A I and Müller-Putz G R 2020 Continuous low-frequency EEG decoding of arm movement for closed-loop, natural control of a robotic arm *J. Neural. Eng.* **17** 046031

Müller-Putz G R *et al* 2016 From classic motor imagery to complex movement intention decoding: the noninvasive Graz-BCI approach *Prog. Brain Res.* **228** 39–70

Müller-Putz G R *et al* 2019 Applying intuitive EEG-controlled grasp neuroprostheses in individuals with spinal cord injury: preliminary results from the moreGrasp clinical feasibility study *2019 41st Annual Int. Conf. IEEE Engineering in Medicine and Biology Society (EMBC)* pp 5949–55

Müller-Putz G R *et al* 2021 Decoding of continuous movement attempt in 2-dimensions from non-invasive low frequency brain signals *2021 10th Int. IEEE/EMBS Conf. on Neural Engineering (NER)* pp 322–5

Müller-Putz G R *et al* 2022 Feel your reach: an EEG-based framework to continuously detect goal-directed movements and error processing to gate kinesthetic feedback informed artificial arm control *Front. Hum. Neurosci.* **16** 110

Müller-Putz G R, Pereira J and Ofner P 2018 Towards non-invasive brain-computer interface for hand/arm control in users with spinal cord injury *Conf. on Brain* (available at: https://ieeexplore.ieee.org/abstract/document/8311498/)

Müller-Putz G, Rupp R and Scherer R 2005 Towards brain controlled movement restoration-part II: application of an asynchronous brain-switch, of ICMP2005 (available at: https://graz.pure.elsevier.com/en/publications/towards-brain-controlled-movement-restoration-part-ii-application)

Mulliken G H, Musallam S and Andersen R A 2008 Decoding trajectories from posterior parietal cortex ensembles *J. Neurosci.* **28** 12913–26

Nichols T E and Holmes A P 2002 Nonparametric permutation tests for functional neuroimaging: a primer with examples *Hum. Brain Mapp.* **15** 1–25

Ofner P and Müller-Putz G R 2012 Decoding of velocities and positions of 3D arm movement from EEG *Conf. Proc.: ... Annual Int. Conf. IEEE Engineering in Medicine and Biology Society. Conf.* vol 2012 pp 6406–9

Ofner P, Schwarz A, Pereira J, Wyss D, Wildburger R and Müller-Putz G R 2019 Attempted arm and hand movements can be decoded from low-frequency EEG from persons with spinal cord injury *Sci. Rep.* **9** 7134

Oldfield R C 1971 The assessment and analysis of handedness: the Edinburgh inventory *Neuropsychologia* **9** 97–113

Pascual-Marqui R D 2002 Standardized low-resolution brain electromagnetic tomography (sLORETA): technical details *Methods Find. Exp. Clin. Pharmacol.* **24** 5–12

Pelli D G 1997 The videotoolbox software for visual psychophysics: transforming numbers into movies *Spat. Vis.* **10** 437–42

Pfurtscheller G, Guger C, Müller G, Krausz G and Neuper C 2000 Brain oscillations control hand orthosis in a tetraplegic *Neurosci. Lett.* **292** 211–4

Pfurtscheller G, Linortner P, Winkler R, Korisek G and Müller-Putz G 2009 Discrimination of motor imagery-induced EEG patterns in patients with complete spinal cord injury *Comput. Intell. Neurosci.* **2009** 104180

Pfurtscheller G, Müller G R, Pfurtscheller J, Gerner H J and Rupp R 2003 "Thought"—control of functional electrical stimulation to restore hand grasp in a patient with tetraplegia *Neurosci. Lett.* **351** 33–36

Pitzalis S, Fattori P and Galletti C 2015 The human cortical areas V6 and V6A *Vis. Neurosci.* **32** E007

Pitzalis S, Sereno M I, Committeri G, Fattori P, Galati G, Tosoni A and Galletti C 2013 The human homologue of macaque area V6A *NeuroImage* **82** 517–30

Pulferer H S *et al* 2021 Learning effects in 2D trajectory inference from low-frequency EEG signals over multiple feedback sessions *Proc. Annual Meeting Austrian Society for Biomedical Engineering* (https://doi.org/10.3217/978-3-85125-826-4-22)

Rohm M, Schneiders M, Müller C, Kreilinger A, Kaiser V, Müller-Putz G R and Rupp R 2013 Hybrid brain-computer interfaces and hybrid neuroprostheses for restoration of upper limb functions in individuals with high-level spinal cord injury *Artif. Intell. Med.* **59** 133–42

Rupp R, Müller-Putz G and Scherer R 2005 Towards brain controlled movement restoration-part I: adaptation of an implantable neuroprosthesis for high spinal cord injured

patients, of ICMP2005 (available at: https://graz.pure.elsevier.com/de/publications/towards-brain-controlled-movement-restoration-part-i-adaptation-o)

Seidler R D, Bo J and Anguera J A 2012 Neurocognitive contributions to motor skill learning: the role of working memory *J. Mot. Behav.* **44** 445–53

Shan H, Xu H, Zhu S and He B 2015 A novel channel selection method for optimal classification in different motor imagery BCI paradigms *Biomed. Eng. Online* **14** 93

Spuler M *et al* 2015 Comparing metrics to evaluate performance of regression methods for decoding of neural signals *2015 37th Annual Int. Conf. IEEE Engineering in Medicine and Biology Society (EMBC)* (https://doi.org/10.1109/embc.2015.7318553)

Tadel F, Baillet S, Mosher J C, Pantazis D and Leahy R M 2011 Brainstorm: a user-friendly application for MEG/EEG analysis *Comput. Intell. Neurosci.* **2011** 879716

Tulsky D S *et al* 2015 Overview of the spinal cord injury–quality of life (SCI-QOL) measurement system *J. Spinal Cord Med.* **38** 257–69

Úbeda A, Azorín J M, Chavarriaga R and R. Millán J D 2017 Classification of upper limb center-out reaching tasks by means of EEG-based continuous decoding techniques *J. Neuroeng. Rehabil.* **14** 9

Velliste M, Perel S, Spalding M C, Whitford A S and Schwartz A B 2008 Cortical control of a prosthetic arm for self-feeding *Nature* **453** 1098–101

Wenderoth N, Debaere F, Sunaert S and Swinnen S P 2005 The role of anterior cingulate cortex and precuneus in the coordination of motor behaviour *Eur. J. Neurosci.* **22** 235–46

Wolpaw J R and McFarland D J 2004 Control of a two-dimensional movement signal by a noninvasive brain-computer interface in humans *Proc. Natl Acad. Sci. USA* **101** 17849–54

Yekutieli D and Benjamini Y 1999 Resampling-based false discovery rate controlling multiple test procedures for correlated test statistics *J. Stat. Plan. Inference* **82** 171–96